Geomorphology 404 (2022) 108183

Contents lists available at ScienceDirect

Geomorphology

journal homepage: www.journals.elsevier.com/geomorphology

Morphological differences of longitudinal profiles between glacial cirques and non-glacial valley heads, described by mathematical fitting

David Krause [a,b,*], Jiří Fišer [c], Marek Křížek [a]

[a] Department of Physical Geography and Geoecology, Faculty of Science, Charles University, Albertov 6, 128 43 Prague 2, Czech Republic
[b] The Krkonoše Mountains National Park Administration, Dobrovského 3, 543 01 Vrchlabí, Czech Republic
[c] Department of Ionosphere and Aeronomy, Institute of Atmospheric Physics, Czech Academy of Sciences, Boční II 1401, 141 31 Prague 4, Czech Republic

ARTICLE INFO

Keywords:
Valley head
Glacial cirque
Longitudinal profile
Function fitting

ABSTRACT

Glacial cirques have specific concave longitudinal profiles different from those of valley heads without glacial imprint. The degree of deepening of valley heads can be used to determine the extent of past mountain glaciation and serve as a tool in palaeoenvironmental reconstructions. The aim of the present paper is to compare longitudinal profiles of glacial cirques and non-glaciated valley heads. For this purpose, we analyzed an alpine area with classic well-developed glacial cirques in the Central Alps (Austria) and a mid-mountain area of the High Sudetes (Czech Republic/Poland) with both cirques and non-glaciated valley heads. We described each valley head by *c*-value function fitting using longitudinal profiles obtained from detailed laser-derived digital elevation models and tested them statistically. The results show, with high accuracy of fitting, significant differences between *c*-values of glacial cirques and those of non-glacial valley heads. This newly presented approach could be useful for distinguishing between valley heads of fluvial origin and glacial cirques, as well as for evaluating the degree of cirque development.

1. Introduction

Cirques are common landforms occurring in mountainous environments, where many valley heads are characterized by the presence of such landform. The spatial distribution and morphometry of glacial cirques provide evidence of cold climates in the past, so they often serve as palaeoenvironmental indicators (Barr and Spagnolo, 2015), especially if they include glacial lakes containing proxy records (e.g., Wick, 2000; Engel et al., 2010; Shala et al., 2014; Vočadlová et al., 2015). From the geomorphological and palaeoglaciological point of view, attention has been paid to cirque allometry (Olyphant, 1981; Evans and Cox, 1995; Brook et al., 2006; Evans, 2006), and several grades of cirque development have been described: classic, well-developed, definite, poor and marginal (Evans and Cox, 1995). Cirque morphometry has usually been described using a multitude of basic to more advanced parameters such as length, width, the L/W ratio, slope, the height ratio and area (e.g., Vilborg, 1984; Evans and Cox, 1995; Hughes et al., 2007; Křížek and Mida, 2013; Mîndrescu and Evans, 2014; Principato and Lee, 2014; Gómez-Villar et al., 2015; Evans and Cox, 2017), that can be extracted from digital terrain models using automatic methods (Spagnolo et al., 2017) in geographic information systems (GIS). Besides these parameters, Haynes (1968) introduced the *k*-curve, which geometrically describes cirque overdeepening and the level of cirque development, and she applied this to study the Scottish Cairngorms Mts; the *k*-curve has been further employed in some other mountain ranges (Brook et al., 2006; Křížek et al., 2012; Seif and Ebrahimi, 2014; Engel et al., 2017). In addition, Křížek et al. (2012) described the properties of the *k*-curve and used it for determining the thickness of sedimentary infills of cirque bottoms or the depth of cirque lakes. The thickness of sedimentary infill estimated by the *k*-curve was confirmed in the Jizerské hory Mts by geophysical means (Engel et al., 2017).

The spatio-temporal development of cirques is variable, and their main erosional activity happens close to the equilibrium line altitude (ELA; Mitchell and Humphries, 2015). As glacier ELA is largely controlled by climate, the history of glacial cirques is a cumulative result of climate dynamics during at least the Quaternary (Barr and Spagnolo, 2015; Barr et al., 2019), and multiple glacial cycles are often believed to be responsible for their development (Gordon, 2001; Brook et al., 2006). Moreover, there are some mid-mountain ranges where cirques occur between fluvial valley heads at similar elevations, so the position of the

* Corresponding author at: Department of Physical Geography and Geoecology, Faculty of Science, Charles University, Albertov 6, 128 43 Prague 2, Czech Republic.
E-mail address: david.krause@natur.cuni.cz (D. Krause).

https://doi.org/10.1016/j.geomorph.2022.108183
Received 29 September 2021; Received in revised form 25 February 2022; Accepted 25 February 2022
Available online 2 March 2022

ELA does not seem to be the only driver of their occurrence; instead, the influence of wind-blown snow accumulation areas (sensu Jeník, 1961) is considered important (Mitchell, 1996; Hassinen, 1998; Křížek et al., 2012; Krause and Margold, 2019). In such mountains of Central Europe, there are still open questions about the glacial history of some valley heads, especially concerning older glacial periods (see Engel et al., 2017; Krause and Margold, 2019). In general, valley heads with different level of glacial traces (sensu Evans and Cox, 1995) should be present in mountain ranges, including some valley heads close to the 'threshold' cirque parameters of the maximum 20° cirque floor slope and a steeper headwall, postulated by Evans and Cox (1974). On the other hand, other valley heads at the same elevations may not show any glacial traces or overdeepening or concavity at all.

The *k*-curve (Haynes, 1968) approach was originally applied to the mid-mountain landscape of the Cairngorms, characterized by planation surfaces and deep-seated valleys. However, glacial cirques in different environments underwent a different glacial development, so for example the Alpine cirques bear many differences compared to the Cairngorms cirques or other lower, isolated mountain ranges. The temporal development of cirques in areas with an extensive glacial history (i.e., cirques covered by ice fields or ice sheets in some phases) differs from that of cirques in areas with dispersed glaciers not exceeding the area of the cirque (Crest et al., 2017; Barr et al., 2019). Moreover, the *k*-curve is not able to identify valley heads with linear longitudinal profiles indicating no past glacial erosional activity.

The aim of this study is to evaluate well-developed as well as medium- and poorly developed glacial valley heads (i.e., cirques) and non-glacial hollows by a unique morphometric parameter that can provide simple information about their longitudinal profiles and help to distinguish between valley heads formed by a glacier and those created by nonglacial geomorphic processes (i.e., mainly fluvial processes). Compared to the older approach (Haynes, 1968), this method uses more effective automatic mathematical function fitting, which should be able to describe a wider range of longitudinal profiles. The value of this parameter should reflect glacial development of the landscape in the past, from well-defined cirques to potentially glaciated valley heads and valley heads where no glacial history is inferred. This approach can be used to help to determine how often/how long for a cirque has been occupied by erosive ice. It is designed for the use of digital elevation models (DEMs) with high spatial resolution, which can be obtained by airborne light detection and ranging (LIDAR) campaigns, which also significantly improves the accuracy of the profile description. For this reason, we selected datasets from two different mountain areas for our study, where such data were available. The first dataset is on mountain valley heads in the High Sudetes with either a glacial or non-glacial history (a non-alpine landscape partly similar to the Cairngorms). The second contains data on typical (well-developed) glacial cirques in the Salzburg and Tirol regions in the Alps.

1.1. Study areas

The first study area is the High Sudetes located on the border between Poland and the Czech Republic (Fig. 1; highest peak Mt. Sněžka, 1603 m a.s.l.). The mountains, which are built of crystalline rocks primarily of Variscian (often termed Hercynian) age (mainly gneiss, mica schist, phyllite, quartzite and granite), have been affected by neotectonic processes related to the Alpine orogeny since the Late Cretaceous, which gave rise to planation surfaces in the summit parts of the mountains. During the Quaternary, there were several cirque and valley glaciers (Křížek et al., 2012), and cosmogenic ^{10}Be exposure dating of

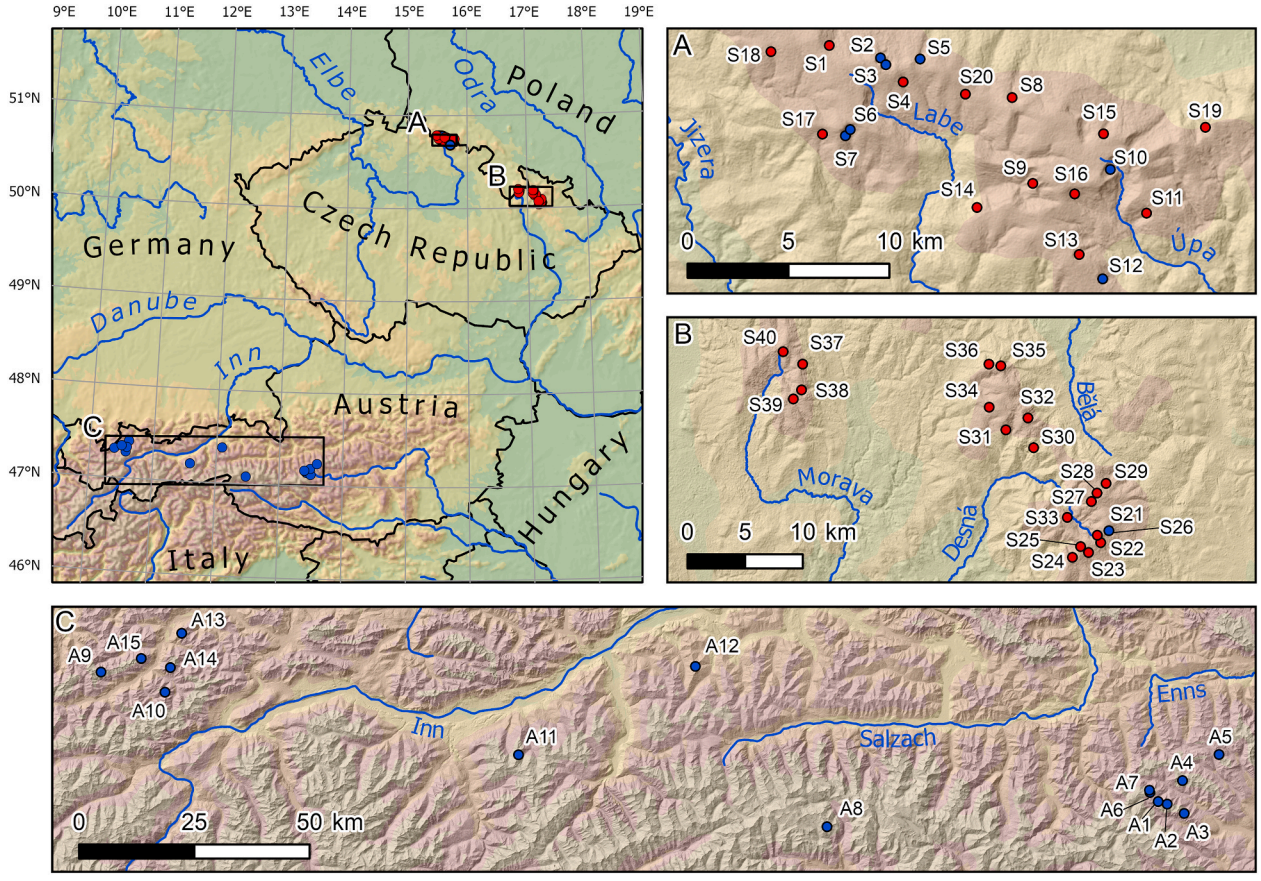

Fig. 1. Locations of studied valley heads. Blue points with black borders for the cirques in the Alps, blue points with grey borders for the cirques in the High Sudetes, and red points with grey borders for the other valley heads in the High Sudetes. For detailed information, see Table 1.

their moraines indicated a MIS 2 age (Engel et al., 2014). The equilibrium line altitude (ELA) during the Last Glacial Maximum (LGM) is expected to have been between 1060 m a.s.l. in the western part of the High Sudetes and 1170 m a.s.l. in the eastern part, and the elevation of the cirques ranges from 1000 to 1500 m a.s.l. (Křížek et al., 2012). Its complex glacial history with a probable greater extent of glaciation, including summit ice caps (Sekyra and Sekyra, 2002) or significantly longer valley glaciers (Carr et al., 2002), has been discussed but not successfully confirmed.

The second study area and validation set of well-developed cirques is located in the Alps (Fig. 1), namely the Tirol and Salzburg regions in Austria. The highest mountain of the region is Mt. Grossglockner (3798 m a.s.l.). The area covers several nappes with different lithological content of both metamorphic and sedimentary origin (most frequently schist, phyllite, gneiss and crystalline limestone). The glacial history is complex, and it has been confirmed that all valleys in the region were covered by glaciers (Ehlers and Gibbard, 2004; Ivy-Ochs et al., 2008; Seguinot et al., 2018). The ELA during the LGM is predicted to be from 1200 to 1500 m a.s.l. (Kelly et al., 2004; Ivy-Ochs et al., 2008) and the current ELA is located between 2700 and 3000 m a.s.l. (Ivy-Ochs et al., 2009 and references therein). The studied glacial cirques are at elevations between 1700 and 2800 m a.s.l. and are not covered by glaciers at present.

2. Methods

2.1. Data and software

The entire procedure of evaluating valley-head longitudinal profiles used in this study consisted of valley head recognition, longitudinal profile tracing and creation, and function fitting for each selected valley head using GIS in ArcMap 10.3 (ESRI, 2015) and function computations in MATLAB (MathWorks, 2019). The source data were LIDAR raster DEMs with 5-m resolution (pixel size) and elevation errors of up to 0.3 m, provided by the Czech State Administration of Land Surveying and Cadastre (www.cuzk.cz) and the Polish Head Office of Geodesy and Cartography (www.gugik.gov.pl) for the High Sudetes and by the Cooperation Open Government Data Österreich (www.data.gv.at) for the Salzburg and Tirol regions in the Alps.

2.2. Valley head recognition and longitudinal profile tracing

Because a valley is a so-called 'fiat object' without physically defined boundaries (Smith and Varzi, 2000), it has always been complicated to find out the exact position along the thalweg (Straumann and Purves, 2011), where a valley head (Crozier, 2004) begins. Tribe (1991, 1992) made the first attempts to extract valley head positions automatically in GIS using a DEM, based on the principle of comparison of relative point elevation (i.e., pixel value) in the surroundings of each cell. In this study, we took a modified approach using a moving window. For the purpose of finding thalwegs and valley heads, the original 5-m DEM was resampled to 40-m pixel size to avoid bias caused by detailed surface morphology of a greater spatial scale than that of valley heads (e.g., shallow channels, anthropogenic landforms). Further, a moving window of 5 × 5 pixels dimensions was passed over the DEM. The raster value resulting from this procedure shows the number of relatively higher cells than the cell in the center of the moving window. A threshold value of minimum 17 was considered for valley-floor cells in the raster. These cells generally occur in a row following the thalwegs of valley network or are located within cirque floors. The threshold value of 17 was set based on comparison of the resulting raster values against the real situation in selected valleys (see Fig. 2). Further, points have been set up in the uppermost valley-floor cells (i.e., pixels having value of 17 or higher), and the pixels at elevations above these points were considered as belonging to the valley heads. These automatically derived valley head points (VHP) have been further used as the lowermost terminal points of longitudinal valley head profiles (Fig. 2). This procedure was applied to the entire study areas (i.e., raster DEM images of the High Sudetes, Tirol and Salzburg regions). For further analyses, only morphologically simple valley heads were chosen. Valley heads with apparent significant influence of lithological or tectonic imprints (i.e., steps, rough surface of slopes), complicated glacial development (i.e., compound and staircase cirques), or visibly huge infill covering the original morphology of the valley head (i.e., glaciers, rock glaciers, screes or colluvial deposits of great thickness) were excluded from the study as well as those infilled by lakes. For example, the surface in the Alps has been exposed to glacial erosion of much greater intensity than in the High Sudetes (Ehlers et al., 2011), which is why compound, staircase, and strongly structurally affected cirques are very common. In the High Sudetes, many valley heads have irregular shape and rugged morphology due to lithological or tectonic imprint. Following the rules mentioned above, excluding valley heads with complicated surfaces, only a relatively small number of valley heads was chosen. In total, we evaluated 55 valley heads based on their longitudinal profiles: 40 in the High Sudetes and 15 in the Alps. The morphology of the selected valley heads allowed us to separate them between glacial (cirque) and non-glacial (generally fluvial), an important distinction which informed the subsequent analysis. In the High Sudetes, we selected both cirques and non-glaciated valley heads. In the Alps, we measured glacial cirques only (see Table 1).

Each profile was traced perpendicularly to the contours between the VHP and the upper limit of each of the 55 valley heads, crossing the part of the valley head with greatest slope inclination (sensu Křížek et al., 2012; see Figs. 2 and 3). This is particularly important in the cases of possibly glaciated valley heads with important fluvial erosion processes that could have potentially levelled the glacial rotation imprint in some parts of the valley heads. Unlike the VHP, the highest elevated point of

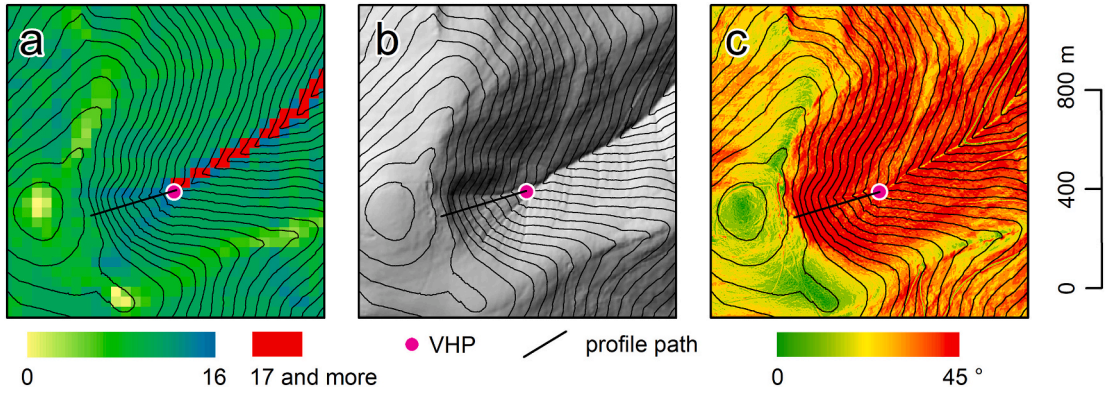

Fig. 2. Valley head point (VHP) detection and profile tracking: (a) VHP initial raster, (b) hillshade raster, (c) slope raster with the steepest path of the profile. The contour interval is 20 m.

Table 1
Studied valley heads with their properties and *c*-values.

ID	Name	Length (m)	Max. elevation (m asl)	Min. elevation (m asl)	Height (m)	L/H	Mean slope (°)	Median slope (°)	Aspect	Glacial cirque (1) / Not confirmed glaciation (0)	*c*-value	RSQ	MSE	Lithology	Latitude	Longitude
S1	Szrenica	267	1233	1123	110	2.430	22.3	23.3	NE	0	−0.81	0.999	0.00005	Granite	50.7885516968	15.5218303233
S2	Mały Śnieżny Kocioł	667	1476	1192	284	2.348	23.0	21.1	NE	1	−1.61	0.989	0.00077	Granite	50.7827848742	15.5577526462
S3	Duży Śnieżny Kocioł	502	1481	1250	231	2.171	24.7	20.9	NE	1	−2.57	0.959	0.00237	Granite	50.779840121	15.5614941636
S4	Martinovka	375	1359	1212	147	2.552	21.4	24.1	SE	0	−0.47	0.999	0.00011	Granite	50.7719856764	15.5736230816
S5	Czarny Kocioł Jagniątkowski	362	1318	1122	196	1.844	28.3	17.4	NE	1	−1.86	0.992	0.00074	Granite	50.7821386311	15.585652815
S6	Malá Kotelní jáma	579	1412	1084	328	1.766	29.4	25.5	SE	1	−0.71	0.998	0.00013	Gneiss	50.7483262575	15.532663619
S7	Velká Kotelní jáma	388	1311	1116	195	1.989	26.6	20.7	SE	1	−2.17	0.980	0.00138	Gneiss	50.7509903518	15.5361149308
S8	Podgórna	267	1260	1139	121	2.207	24.3	25.2	NE	0	−0.45	0.999	0.00008	Granite	50.7646607736	15.6499360675
S9	Lovecký důl	719	1452	1037	415	1.732	29.8	34.4	SW	0	−0.15	0.998	0.00017	Gneiss	50.7264588306	15.6640805027
S10	Úpská jáma	493	1413	1106	307	1.607	31.7	26.9	E	1	−0.54	0.993	0.00060	Granite	50.732246715	15.7185371906
S11	Růžový důl	402	1256	1014	242	1.661	30.9	32.7	W	0	−0.06	0.997	0.00031	Gneiss	50.712754554	15.7435628822
S12	Vlčí jáma	368	1161	994	167	2.201	24.4	18.9	E	1	−1.03	0.999	0.00001	Gneiss	50.6945660623	15.6960503358
S13	Liščí jáma	436	1323	1135	188	2.319	23.3	21.5	E	0	−0.43	0.995	0.00034	Gneiss	50.715923974	15.6246904338
S14	Černá strouha	341	1110	924	186	1.834	28.5	31.9	N	0	−0.4	0.999	0.00012	Gneiss	50.7482460966	15.713964062
S15	Biały Jar	398	1378	1192	186	2.138	25.0	28.1	NE	0	−0.67	0.998	0.00014	Granite	50.7215712032	15.6933489013
S16	Modrý důl	710	1505	1236	269	2.639	20.7	21.7	S	0	0.23	0.998	0.00018	Gneiss	50.7491557352	15.5166791336
S17	Dvoračky	573	1277	1073	204	2.807	19.6	23.0	S	0	−0.45	0.999	0.00006	Gneiss	50.785920216	15.4807871001
S18	Lubošská jáma	141	1200	1153	47	2.989	18.5	23.5	S	0	−1.11	0.991	0.00089	Granite	50.7506041047	15.785602996
S19	Sowia dolina	504	1208	950	258	1.953	27.0	27.3	NW	0	−0.1	0.998	0.00014	Gneiss	50.7663300706	15.6171628382
S20	Dírečka	422	1161	1097	64	6.592	8.6	9.7	S	0	0.12	0.999	0.00008	Granite	50.6836304525	15.7125114962
S21	Velká kotlina	293	1338	1155	183	1.601	31.8	32.9	SE	1	−0.92	0.999	0.00011	Phylitte	50.0563735138	17.2367797406
S22	Mezikotlí	468	1328	1185	143	3.273	17.0	15.0	SE	0	−0.71	0.971	0.00208	Phylitte	50.0472864907	17.2264927599
S23	Malá kotlina	410	1303	1117	186	2.204	24.4	22.1	S	0	−0.61	0.996	0.00038	Phylitte	50.0398612945	17.2114046482
S24	Jelení příkop	358	1333	1095	238	1.503	33.3	34.0	NW	0	0.09	0.988	0.00118	Phylitte	50.0363920235	17.1919008964
S25	Jelení hřbet	306	1282	1117	165	1.855	28.2	32.5	NW	0	0.14	1.000	0.00004	Phylitte	50.044576807	17.2020414981
S26	Medvědí důl	270	1381	1248	133	2.028	26.2	27.2	W	0	0.29	0.998	0.00023	Phylitte	50.0529673167	17.2228275725
S27	Divoký důl	218	1341	1270	71	3.063	18.1	19.3	W	0	0.38	0.998	0.00019	Gneiss	50.0795236111	17.2166634148
S28	Česnekový důl	438	1425	1297	128	3.423	16.3	16.5	N	0	−0.03	0.996	0.00042	Gneiss	50.0859608697	17.2238370885
S29	Střední Opava	887	1316	966	350	2.533	21.5	22.2	NE	0	−0.24	1.000	0.00003	Gneiss	50.0931542675	17.2353542299
S30	Koutský žleb	239	989	908	81	2.946	18.7	19.2	SW	0	0.27	0.992	0.00079	Gneiss	50.1226416361	17.1486096622
S31	Klínová hora	524	1145	915	230	2.277	23.7	25.8	SE	0	−0.61	0.992	0.00075	Gneiss	50.1371440616	17.115550683
S32	Sněžná kotlina	686	1274	920	354	1.938	27.2	26.8	E	0	−0.44	1.000	0.00003	Gneiss	50.1458646808	17.1426773781
S33	Jezerná	316	1231	1022	209	1.511	33.2	33.9	E	0	−0.15	0.999	0.00008	Gneiss	50.0675176049	17.1870891235
S34	Hučava	560	1284	1114	170	3.295	16.9	16.8	W	0	0.06	1.000	0.00003	Gneiss	50.1552716465	17.096174735
S35	Šeráčká kotlina	473	1319	1053	266	1.777	29.2	31.6	E	0	−0.39	0.996	0.00037	Gneiss	50.1872368264	17.1115993509
S36	Vražedný potok	291	1171	1024	147	1.980	26.7	27.6	N	0	−0.02	0.999	0.00011	Gneiss	50.1887623186	17.0973946521
S37	Stříbrnický potok	271	1149	1021	128	2.116	25.2	27.0	E	0	−0.11	0.997	0.00027	Gneiss	50.1924972926	16.8710631766
S38	Sušina	498	1271	1002	269	1.852	28.2	28.6	E	0	−0.32	0.999	0.00012	Gneiss	50.172604104	16.8688499686
S39	Prudký potok	588	1258	1151	107	5.496	10.3	8.8	SE	0	−0.89	0.991	0.00085	Gneiss	50.1657295988	16.8587995139
S40	Morava	350	1324	1149	175	1.999	26.5	29.7	SW	0	0.2	0.995	0.00045	Gneiss	50.2028052268	16.8476535061
A1	Soliesingalm	437	2204	1914	290	1.507	33.3	33.4	N	1	−0.34	0.998	0.00014	Schist	47.1442314661	13.4212740873
A2	Pleissnitz	274	2334	2191	143	1.916	27.5	30.0	N	1	−2.87	0.986	0.00103	Schist	47.1394494768	13.4471883176
A3	Kocheralm	433	2265	2024	241	1.797	29.0	31.3	N	1	−1.37	0.996	0.00030	Schist	47.1220113274	13.4965474074
A4	Schieferalm	305	2540	2291	249	1.225	38.6	45.8	S	1	−1.07	0.990	0.00101	Schist	47.1858956033	13.4896438353
A5	Wirpitsch	392	2192	1965	227	1.727	29.9	39.4	E	1	−0.83	0.995	0.00047	Gneiss	47.2379649971	13.5931580344
A6	Weisseck 1	455	2697	2252	445	1.022	43.1	34.2	NE	1	−2.08	0.986	0.00093	Schist	47.1613514348	13.3973170319
A7	Weisseck 2	451	2690	2392	298	1.513	33.2	36.7	NE	1	−0.32	0.989	0.00083	Ophiolite	47.1656532492	13.3958971985

(*continued on next page*)

Table 1 (*continued*)

ID	Name	Length (m)	Max. elevation (m asl)	Min. elevation (m asl)	Height (m)	L/H	Mean slope (°)	Median slope (°)	Aspect	Glacial cirque (1) / Not confirmed glaciation (0)	*c*-value	RSQ	MSE	Lithology	Latitude	Longitude
A8	Raneburgkogel	531	2770	2517	253	2.099	25.4	22.4	S	1	−2.3	0.998	0.00014	Schist	47.0781906467	12.4770082313
A9	Birgerkar	504	2457	2252	205	2.459	22.1	26.8	S	1	−2.12	0.979	0.00200	Marl	47.3140820569	10.3828505513
A10	Hochgwas	378	2326	2012	314	1.204	39.0	32.5	N	1	−1.04	0.995	0.00041	Crystalline limestone	47.2821945751	10.5684466984
A11	Seekar	513	2650	2319	331	1.550	32.6	28.4	SE	1	−1.1	0.996	0.00032	Phylitte	47.1954660603	11.5884696531
A12	Feldalphorn	232	1858	1762	96	2.417	22.4	25.7	E	1	−0.95	0.999	0.00012	Marl	47.3814418955	12.0848811765
A13	Hühnerspiel	298	2037	1907	130	2.292	23.5	18.3	N	1	−2.18	0.986	0.00127	Marl	47.3988992363	10.6067062418
A14	Stablsee	355	2302	2035	267	1.330	36.5	32.1	N	1	−1.69	0.985	0.00106	Crystalline limestone	47.3311731747	10.5804547805
A15	Grosskar	587	2410	2017	393	1.494	33.5	32.7	SE	1	−2.29	0.996	0.00030	Marl	47.3452855813	10.4955457341

each profile was set manually as the upper limit of each valley head, situated in different position relative to surrounding landforms (e.g., ridges, summit planation surfaces) and following local conditions in the places where there is a break of slope and curvature (see Figs. 2 and 3). Profile elevation values were obtained from the 5-m DEMs. Basic morphometric and other interesting data were obtained for each profile (i.e., maximal elevation, minimal elevation, height, length, the L/H ratio, median slope, aspect, and lithology obtained from local geological maps).

2.3. Function fitting

All profiles were normalized (sensu Demoulin, 1998), so they were plotted with both x and y values ranging from 0 to 1. For these normalized profiles, the fitting of the function

$$(1 - \mathrm{x})exp.\mathrm{cx},$$

where *x* is the profile value and *c* is the variable coefficient, was applied. The variable *c* describes the shape of the longitudinal profile. The more negative the value of the *c* coefficient (hereinafter referred to as the *c*-value), the greater the deepening of the profile in terms of the potential rotational ice flow imprint. The reliability of function fitting of each profile is described by the RSQ and MSE error values (see the MATLAB Documentation; MathWorks, 2019). RSQ stands for the square of the correlation between the fitted values and the data values; it ranges from 0 to 1, the value of 1 meaning that the function fits perfectly. MSE is the mean of squared errors and reflects the average deviation of the values from the fit to the data values. The lower the value of MSE, the better the fit.

2.4. Statistical analysis

We evaluated the set of profiles using a histogram of *c*-values to see whether there were any groups of profiles with similar *c*-values. We then plotted *c*-values and profile heights (the only two features without significant correlations, tested using Pearson's correlation coefficient: the *c*-value and profile height; Table 2) to outline the pattern of relationships and differences between the valley heads. One-way analysis of variance (ANOVA) was applied to *c*-values of valley heads of glacial origin and those of other valley heads of non-glacial origin. The result was then tested using an F-test at the significance level of $p = 0.05$. All statistical analyses were performed using STATISTICA 9.0 (StatSoft, 2009).

3. Results

3.1. Basic morphometric variables/features of studied profiles

We selected a total of 55 valley heads in the High Sudetes and the Alps for analysis, 23 of which are glacial cirques (Table 1). The maximum and minimum elevations of the entire group of profiles are 2770 m a.s.l. and 908 m a.s.l., respectively. The length of the profiles ranges from 140.5 to 886.7 m, with an average of 427.24 m. The height of the valley heads varies between 47 and 445 m, and the average vertical difference of the valley heads analyzed is 213.8 m. The computed L/H ratio is between 1.022 and 6.592, with an average of 2.218, and the mean slope is between 8.6 and 43°, the average being 26.18° (Table 1).

Comparison of basic characteristics of the profiles located in the Alps and in the High Sudetes revealed no crucial differences in profile length, which is on average 456.3 m for glacial cirques in the High Sudetes and 409.6 m in the Alps. The average length of non-glacial valley heads in the High Sudetes is 428.2 m. The average height of 258.8 m for the cirques in the Alps is comparable to the average of the cirques in the High Sudetes (236.3 m) but stands in contrast with the value of only 187 m for the other valley heads in the High Sudetes. Also, the L/H ratio of cirques is lower, with an average of 1.703 in the Alps and 1.940 in the High Sudetes, contrasting with 2.528 for the other valley heads in the

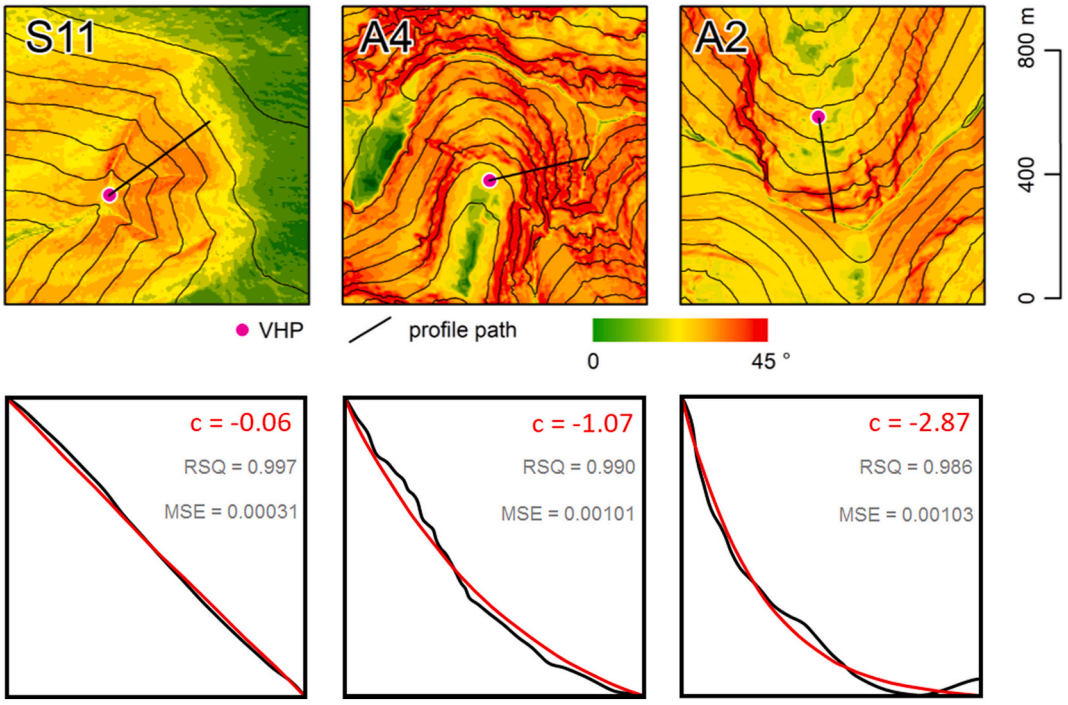

Fig. 3. Examples of selected valley heads and their *c*-values.

Table 2
Correlation table of basic morphometric parameters of the valley heads showing the values of the Pearson correlation coefficient.

	Length	Height	L/H	Mean slope	*c*-value
Length	1	**0.67**	0.08	−0.07	−0.02
Height	**0.67**	1	**−0.57**	**0.67**	−0.2
L/H	0.08	**−0.57**	1	**−0.89**	0.22
Mean slope	−0.07	**0.67**	**−0.89**	1	−0.24
***c*-value**	−0.02	−0.2	0.22	−0.24	1

High Sudetes. The average slope for the cirques in the Alps is 31.3°, for the cirques in the High Sudetes 27.4°, again in contrast to the value of 23.4° of the other valley heads in the High Sudetes. As shown above, when we compared cirque profiles from the High Sudetes with those in the Alps, their morphometric values did not differ substantially (Table 1). On the contrary, the values of the other valley heads in the High Sudetes show differences from those of glacial origin.

3.2. Values of c for the studied profiles

We expressed profile deepening using the *c*-value (see Table 1). The RSQ and MSE parameters show successful fit goodness of the function among all profiles, giving the lowest RSQ of 0.959 (average 0.994) and the highest MSE of 0.00237 (average: 0.0005). The average *c*-value for the whole group of profiles is −0.76, and the highest and lowest values are 0.38 and −2.87, respectively. The average *c*-value of the cirques is −1.5 in the Alps and −1.43 in the High Sudetes; on the contrary, non-glacial valley heads in the High Sudetes have an average *c*-value of −0.245, which is notably different (Fig. 4). The average *c*-value for the entire group cirques (−1.47) is considerably lower than the average of the rest of the group (−0.245). The difference between these two groups is supported by ANOVA (Fig. 5), which demonstrates that cirques differ significantly from other valley heads (non-glacial origin) by their *c*-values. Regardless, some cirques do have relatively high *c*-values, both in the High Sudetes (e.g., S6: −0.71, S10: −0.54) and in the Alps (e.g., A1: −0.34, A7: −0.32), but those are not abundant. The four best-developed cirques in the High Sudetes (S2, S3, S5 and S7) have lower *c*-values than the Alpine average of −1.5. Moreover, the S3 profile has the second lowest *c*-value in the entire group of profiles and can be considered a very well-developed cirque. On the other hand, there are many profiles with *c*-values around zero and even above zero (S9, S11, S16, S19, S20, S24, S25, S26, S27, S28, S30, S33, S34, S36, S37 and S40; all of these profiles have *c*-values of −0.15 or greater, in 8 cases positive; see Table 1). None of these profiles are located in valley heads of glacial origin, and all of them are of fluvial origin with no significant deepening. Moreover, some of the profiles do not have confirmed glaciation, although their concavity is greater than in the cases of ordinary fluvial valley heads (notably S1, S18, S22, S23, S31, S39; average c −0.79), though other processes, such as landslides, could have caused this.

A plot of non-autocorrelated variables, *c*-values and profile height (Table 2), shows that the best-developed cirques are located in the left sector (Fig. 6) whereas the fluvial valley heads are on the right. Some cirques are plotted in the middle of the plot, surrounded by other valley heads of non-glacial origin (Fig. 6), which means that no threshold is made between those groups, but a zone of overlapping *c*-values between these categories is observed. The cirques within this zone usually have a greater height compared to the other valley heads. Possible straight discriminator line passing through *c*-value −1 for profiles 100 m high and −0.5 for profiles 300 m high would divide the groups of cirques and other valley heads with onlaaaaay 4 exceptions: S32 (a non-cirque between cirques), and A1, A7, and A12 (cirques between non-cirques).

4. Discussion

4.1. Usefulness of the c-value

The *c*-value is designed to describe longitudinal profiles of valley heads by a unique number with the ability to fit an existing surface with very high accuracy. This is achieved by function fitting, and the very strong similarity of the resulting *c*-value curves to the real surface profiles is confirmed by the MSE and RSQ values (Fig. 3). Starting at the top of the valley head/cirque crest and ending at the VHP, the *c*-value is mainly a mathematical expression of the profile deepening related to the straight line between the uppermost point of the profile and the VHP,

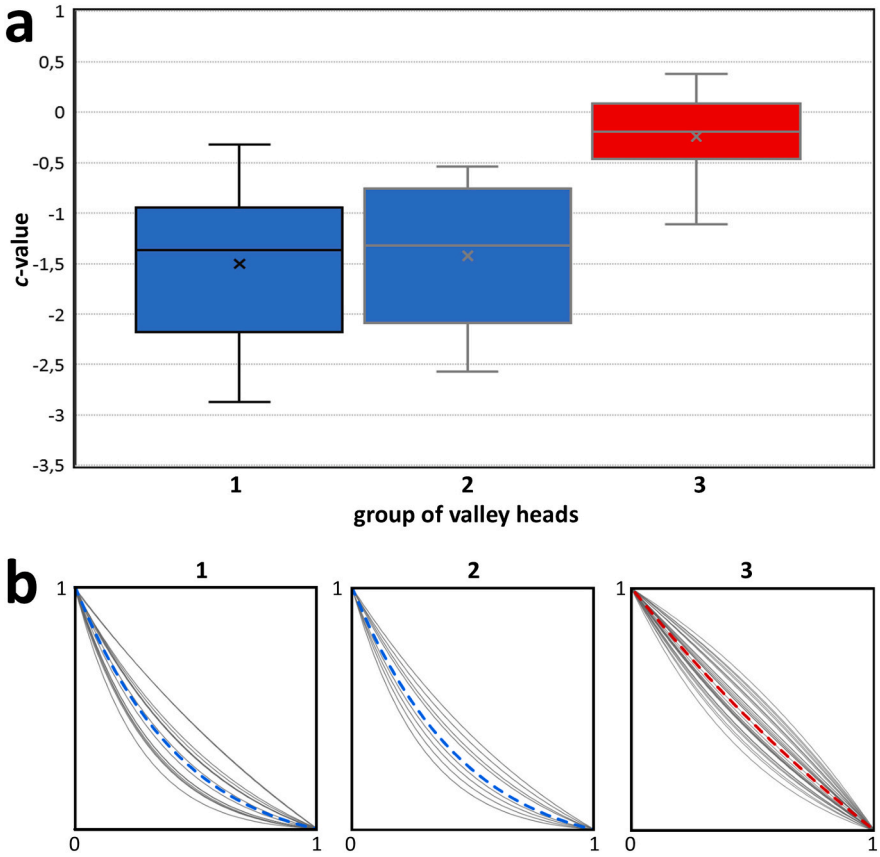

Fig. 4. Boxplots of the c-values of the cirques in the Alps (1), the cirques in the High Sudetes (2) and the other valley heads in the High Sudetes (3) (a). The fitted curves for the *c*-value calculation printed for the same groups as in a (b).

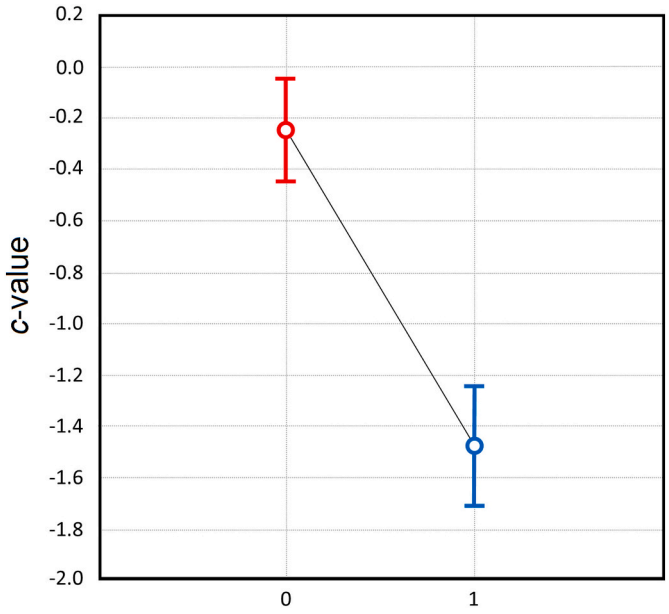

Fig. 5. Significant differences in *c*-values between glacial cirques (1) and other valley heads (0) described by ANOVA. Vertical bars in a denote the 0.95 confidence interval on the mean value.

which is 45° in the case of profiles normalized after Demoulin (1998): the *c*-value of 0 is expressed by this straight line. If a cirque is overdeepened, then the VHP and so the terminating point of the profile is located in the hollow. Therefore, the *c*-value is expressed by a simple decreasing arc-shaped profile, so it is able to describe and classify overdeepened cirques as well as linear fluvial valley heads with nearly the same accuracy of function fitting.

On the other hand, the *k*-curve (described by a unique number as well), introduced by Haynes (1968) and frequently used to describe cirque profile overdeepening (Brook et al., 2006; Křížek et al., 2012; Seif and Ebrahimi, 2014; Engel et al., 2017), reflects the shape of the cirque floor perceptibly (i.e., it describes longer profile than the *c*-value: decreasing to the VHP at the cirque floor and then rising up to the cirque limit in the case of overdeepened cirques). From the principle of its shape, the *k*-curve always expresses the deepening of a profile, so it is not able to fit the linear profile of a typical fluvial valley head. Although there is a method to derive the *k*-curve value mathematically using cirque morphometric parameters (Křížek et al., 2012), there are still no indicators of the accuracy of the description, meaning that equivalents to the *c*-value MSE and RSQ are missing.

For the best reliable results, the *k*-curve should be applied to the original erosional shape of the cirque developed in bedrock and not include overlying sediments. In the case of cirques, the *c*-value used in this study, which represents profile deepening, reflects the morphology of the headwall and a part of the cirque floor, as it describes the profile which is retained through the steepest part of the headwall, with termination at the VHP located within the cirque floor. According to Evans and Cox (1974), cirque floors should have slope gradients of less than 20°, which might fail to take into account floor overdeepening, but possibly with significant imprint of glacial erosion in their profile morphology. Olyphant (1977), Brook et al. (2006), and Benn and Evans (2014) demonstrate that the cirque headwall erosion rates are usually 1.5–13 times greater than the cirque floor deepening rates, so the morphology of the profiles terminating at the VHP (expressed by a *c*-value) should reflect the past glacial imprint and the level of cirque

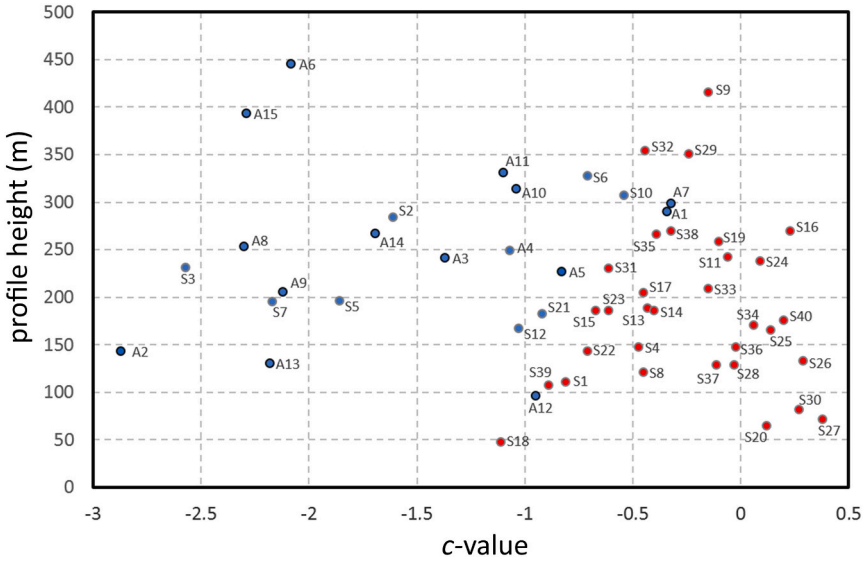

Fig. 6. Plot of the *c*-values and the profile height. Glacial cirques are colored blue, other valley heads are colored red; grey borders delineate the Sudetes, black borders the Alps.

development very well, especially in the cases of poorly developed (not overdeepened) cirques with possibly shorter duration of glacial erosion (i.e., marginal cirques sensu Evans, 2006; Fig. 4d, page 252). However, Sanders et al. (2013) documented roughly equivalent erosion rates for the headwall retreat and vertical incision of a presently glaciated, well-developed cirque in British Columbia over 50 years, so the presumption of faster headwall retreat is obviously not applicable in general.

As each headwall is an erosional landform with a relatively steep slope gradient, any influence of thick sediment covering the erosional bedrock profile is expected to be relatively rare, especially when the profile is set through the steepest part of the headwall. Even so, the headwall is subjected to postglacial erosional processes, and some taluses or screes often occupy the headwall foot and occasionally reach even higher positions of the headwall, which could affect the topography-derived profile and thus the *c*-value. For this reason, it is necessary to avoid the tracing of profiles over huge sedimentary accumulations at headwall feet in order to obtain the most original shape of the uncovered headwall and its transition to the floor. However, when deriving profiles from a topographical surface (expressed by a DEM), it is still easier to find cirque headwalls and floors without significant sedimentary cover than infilled bedrock-based cirque floors for the usage of the *k*-curve (sensu Haynes, 1968). The *c*-value could also be useful for characterizing cirques affected by other processes (e.g., fluvial erosion, mass wasting), where only part of the original cirque headwall remained. In a few cases, the concave shape of a longitudinal profile of a valley head (i.e., having a negative *c*-value) could be a result of certain processes other than glaciation (see Young, 2004), with the complication that in some cases even a classic glacial cirque might have developed superimposed on another landform, for example a landslide (Turnbull and Davies, 2006). Nevertheless, the almost exclusive factor of cirque development worldwide is the glacier action (Evans, 2020). This should always be taken into account, and local geological and geomorphological settings must be studied when interpreting morphometric results. Because the *c*-value mainly reflects the profile, it is well useable for well-developed overdeepened cirques, as well as for poorly developed cirques with a steep cirque floor, or fluvial valley heads. In the future, it could be a helpful tool for settling doubts regarding the origin of valley heads with equivocal evidence of past glaciation.

4.2. Profile deepening as a past glacial imprint

It is assumed that cirque deepening and dimensions are a result of glacial erosion, mainly rotational ice flow over very long time periods (Brook et al., 2006). More negative *c*-values (i.e., greater profile deepening) reflect more pronounced glacial shaping of valley heads (sensu Evans and Cox, 1995). Our results indicate that the cirques in this study mostly correspond to this assumption (Table 1). On the other hand, valley heads where the presence of past glaciers is not assumed have *c*-values near zero, which means that the profile is not deepening at all. Because the deepening and overdeepening of the cirques is mainly a function of the time of glacial occupation in the past (Brook et al., 2006; Barr and Spagnolo, 2015), the final cirque vertical dimensions (and possibly the *c*-value) may be different between two locations with similar length of glacial occupation but different lithology (Evans, 2006). Most of the studied valley heads are located in crystalline rock areas (except for A9, A12, A13, and A15 developed in marls), so the weathering properties of the rocks could be comparable. Thus, the presumption of positive feedback between the duration of glacial occupation and profile concavity could be used for discussing the results obtained from the entire dataset considered in this study. The resulting *c*-values identify many well-developed cirques especially in the Alps, but also in the High Sudetes (Table 1, Fig. 6).

According to the assumptions of Brook et al. (2006) and Gordon (1977), very well developed cirques, in this study with *c*-values of around −2, should have experienced the longest past glacial occupation (erosional activity) among the studied cirques and it might take longer than five hundred thousand years of total glacial occupation to achieve such a low *c*-value. This could be the case of at least six cirques in the Alps (A2, A6, A8, A9, A13 and A15) and three cirques in the High Sudetes (S3, S5 and S6). These cirques could be considered classic cirques sensu Evans and Cox (1995). Cosmogenic ^{10}Be exposure dating of moraines in the High Sudetes indicates at least a last glacial period age (MIS 1 and 2; Engel et al., 2014), but the morphometry of erosional landforms behind the moraines (i.e., profile deepening described in this study or in Křížek et al., 2012) shows that the total intermittent occupation of a cirque by an eroding glacier might have been longer than one glacial period (sensu Brook et al., 2006). Although the High Sudetes have many fewer cirques, have lower elevations, and had a lesser extent of paleoglaciers than the Alps, the best-developed cirques in the High Sudetes have similar *c*-values as the best-developed Alpine cirques in the study dataset (Fig. 6). This could be explained by several hypotheses, and further research is needed to reveal the detailed glacial history of the study sites. The different lengths of cold- or warm-based glacier preservation or glacial extent across the cirque borders seems to be a

crucial factor. It is assumed that the cirques did not develop during ice cap or ice field occupation (Jansson et al., 1999; Barr et al., 2019), which is the case of the Alps at LGM. Thus, different climatological conditions during glacial periods, which controlled glacier basal temperature, and their variations between the study sites could have played a significant role in cirque development. However, it is also possible that cirques reached their 'mature' profile after a set amount of time of occupation by an erosional, warm based glacier, which occurred at both sites earlier on in the Quaternary, and then changed little over subsequent glaciations (Barr et al., 2019; Spagnolo et al., 2022).

The other documented group of cirques has *c*-values between −0.32 and −1.69, but usually around −1. These cirques still show much greater deepening than fluvial valley heads, and most of them could be considered well-defined or definite cirques sensu Evans and Cox (1995). Only the S10, A1 and A7 cirques, having a *c*-value of −0.54 and greater, seem to be categorized as poor or marginal cirques (sensu Evans and Cox, 1995). The *c*-value of −0.5 describes a slightly deepened profile, but it does not indicate cirques unequivocally, as even some fluvial valley heads without a documented glacial history have similar *c*-values. On the other hand, possible glacial occupation or intensive nivation of valley heads with *c*-values of −0.5 and slightly greater during some more extensive glacial periods cannot be ruled out. The last group of valley heads without visible profile concavity (*c*-values of −0.15 and greater) bear no signs of erosional glacial imprint whatsoever and represents fluvial valley heads.

5. Conclusions

We examined the profiles of 55 valley heads in the High Sudetes and the Alps using simple function fitting from which a *c*-value could be calculated. This is a parameter that effectively describes longitudinal profile deepening of dimensionless normalized profiles (Demoulin, 1998) by a unique number. A *c*-value of zero means a linear profile; the more negative the *c*-value, the deeper the profile it describes. All glacial cirques considered in this study (i.e., 8 sites in the Sudetes and 15 sites in the Alps) exhibit negative *c*-values with an average of −1.4, which we interpret as an indication that these cirques were occupied by eroding glaciers during multiple glaciations. Furthermore, there are numerous recognized fluvial valley heads without glacial deepening (16 sites in the High Sudetes having *c*-values equal to or greater than −0.15). Beside those, some valley heads having *c*-values of around −0.2 or even lower are present in the High Sudetes. Some of them could possibly represent poorly developed cirques or slightly concave fluvial valley heads.

The *c*-value approach works well in different types of mountain ranges, so it is applicable in both alpine and non-alpine landscapes. Compared to the *k*-curve (defined by Haynes, 1968), the *c*-value is able to fit the actual surface better. The approach works well together with remotely sensed elevation data. While headwall morphology is crucial for its computation, it is not necessary to know the position of the deepest point of the glacial cirque floor hidden under sediments or water, which, on the other hand, is a requirement for the correct calculation of the *k*-curve. Moreover, the profile described by the *c*-value helps to describe the level of development of cirques (sensu Evans and Cox, 1995). This could further be used for revealing their geomorphic history, specifically the intensity and duration of past glacial erosion episodes, through a single or multiple glaciation(s).

The *c*-value method is very simple and accurate in evaluating the morphology of valley heads and could be helpful in distinguishing between glacial cirques and other valley heads. As it is easily applicable in every kind of landscape (i.e., alpine mountain ranges or even ranges with summit flats) and suitable for use with digital elevation models, it is a universal tool for analyzing valley heads anywhere.

Declaration of competing interest

The authors declare that they have no known competing financial interests or personal relationships that could have appeared to influence the work reported in this paper.

Acknowledgments

The authors thank Ian S. Evans and Matteo Spagnolo for their constructive comments and suggestions on the manuscript.

References

Barr, I.D., Spagnolo, M., 2015. Glacial cirques as palaeoenvironmental indicators: their potential and limitations. Earth Sci. Rev. 151, 48–78. https://doi.org/10.1016/j.earscirev.2015.10.004.

Barr, I.D., Ely, J.C., Spagnolo, M., Evans, I.S., Tomkins, M.D., 2019. The dynamics of mountain erosion: cirque growth slows as landscapes age. Earth Surf. Process. Landf. 44, 2628–2637. https://doi.org/10.1002/esp.4688.

Benn, D., Evans, D.J., 2014. Glaciers and Glaciation. Routledge.

Brook, M.S., Kirkbride, M.P., Brock, B.W., 2006. Cirque development in a steadily uplifting range: rates of erosion and long-term morphometric change in alpine cirques in the Ben Ohau Range, New Zealand. Earth Surf. Process. Landf. 31, 1167–1175. https://doi.org/10.1002/esp.1327.

Carr, S., Engel, Z., Kalvoda, J., Parker, A., 2002. Sedimentary evidence for extensive glaciation of the Úpa valley, Krkonoše Mountains, Czech Republic. Z. Geomorphol. 46, 523–537. https://doi.org/10.1127/zfg/46/2002/523.

Crest, Y., Delmas, M., Braucher, R., Gunnell, Y., Calvet, M., Aster Team, 2017. Cirques have growth spurts during deglacial and interglacial periods: evidence from 10Be and 26Al nuclide inventories in the central and eastern Pyrenees. Geomorphology 278, 60–77. https://doi.org/10.1016/j.geomorph.2016.10.035.

Crozier, M., 2004. Hillslope hollow. In: Goudie, A.S. (Ed.), Encyclopedia of Geomorphology. Routledge, London, pp. 521–524.

Demoulin, A., 1998. Testing the tectonic significance of some parameters of longitudinal river profiles: the case of the Ardenne (Belgium, NW Europe). Geomorphology 24, 189–208. https://doi.org/10.1016/S0169-555X(98)00016-6.

Ehlers, J., Gibbard, P.L., 2004. Quaternary Glaciations-extent and Chronology: Part I: Europe. Elsevier.

Ehlers, J., Ehlers, J., Gibbard, P., Hughes, P., 2011. Quaternary Glaciations-extent and Chronology: A Closer Look. Elsevier.

Engel, Z., Nývlt, D., Křížek, M., Treml, V., Jankovská, V., Lisá, L., 2010. Sedimentary evidence of landscape and climate history since the end of MIS 3 in the Krkonoše Mountains, Czech Republic. Quat. Sci. Rev. 29, 913–927. https://doi.org/10.1016/j.quascirev.2009.12.008.

Engel, Z., Braucher, R., Traczyk, A., Laetitia, L., AsterTeam, 2014. 10Be exposure age chronology of the last glaciation in the Krkonoše Mountains, Central Europe. Geomorphology 206, 107–121. https://doi.org/10.1016/j.geomorph.2013.10.003.

Engel, Z., Křížek, M., Kasprzak, M., Traczyk, A., Hložek, M., Krbcová, K., 2017. Geomorphological and sedimentary evidence of probable glaciation in the Jizerské hory Mountains, Central Europe. Geomorphology 280, 39–50. https://doi.org/10.1016/j.geomorph.2016.12.008.

ESRI, 2015. ESRI: ArcMap 10.3. https://support.esri.com/en/products/desktop/arcgis-desktop/arcmap/10-3-1.

Evans, I.S., 2006. Allometric development of glacial cirque form: geological, relief and regional effects on the cirques of Wales. Geomorphology 80, 245–266. https://doi.org/10.1016/j.geomorph.2006.02.013.

Evans, I.S., 2020. Glaciers, rock avalanches and the 'buzzsaw' in cirque development: why mountain cirques are of mainly glacial origin. Earth Surf. Process. Landf. https://doi.org/10.1002/esp.4810.

Evans, I.S., Cox, N.J., 1974. Geomorphometry and the operational definition of cirques. Area 150–153.

Evans, I., Cox, N.J., 1995. The form of glacial cirques in the English Lake District, Cumbria. Z. Geomorphol. 39, 175–202. https://doi.org/10.1127/zfg/39/1995/175.

Evans, I.S., Cox, N.J., 2017. Comparability of cirque size and shape measures between regions and between researchers. Z. Geomorphol. Suppl. 61, 81–103. https://doi.org/10.1127/zfg_suppl/2016/0329.

Gómez-Villar, A., Santos-González, J., González-Gutiérrez, R.B., Redondo-Vega, J.M., 2015. Glacial cirques in the southern side of the cantabrian mountains of southwestern europe. Geogr. Ann. Ser. A 97, 633–651. https://doi.org/10.1111/geoa.12104.

Gordon, J.E., 1977. Morphometry of cirques in the Kintail-Affric-Cannich area of Northwest Scotland. Geogr. Ann. Ser. A 59, 177–194. https://doi.org/10.1080/04353676.1977.11879950.

Gordon, J.E., 2001. The corries of the cairngorm mountains. Scott. Geogr. J. 117, 49–62. https://doi.org/10.1080/00369220118737110.

Hassinen, S., 1998. A morpho-statistical study of cirques and cirque glaciers in the Senja-Kilpisjärvi area, northern Scandinavia. Nor. Geol. Tidsskr. 52, 27–36. https://doi.org/10.1080/00291959808552381.

Haynes, V.M., 1968. The influence of glacial erosion and rock structure on corries in Scotland. Geogr. Ann. Ser. A 50, 221–234. https://doi.org/10.1080/04353676.1968.11879785.

Hughes, P.D., Gibbard, P.L., Woodward, J.C., 2007. Geological controls on Pleistocene glaciation and cirque form in Greece. Geomorphology 88, 242–253. https://doi.org/10.1016/j.geomorph.2006.11.008.

Ivy-Ochs, S., Kerschner, H., Reuther, A., Preusser, F., Heine, K., Maisch, M., Kubik, P.W., Schlüchter, C., 2008. Chronology of the last glacial cycle in the European Alps. J. Quat. Sci. 23, 559–573. https://doi.org/10.1002/jqs.1202.

Ivy-Ochs, S., Kerschner, H., Maisch, M., Christl, M., Kubik, P.W., Schlüchter, C., 2009. Latest Pleistocene and Holocene glacier variations in the European Alps. Quat. Sci. Rev. 28, 2137–2149. https://doi.org/10.1016/j.quascirev.2009.03.009.

Jansson, P., Richardson, C., Jonsson, S., 1999. Assessment of requirements for cirque formation in northern Sweden. Ann. Glaciol. 28, 16–22. https://doi.org/10.3189/172756499781821959.

Jeník, J., 1961. Alpinská vegetace Krkonoš, Králického Sněžníku a Hrubého Jeseníku: teorie anemo-orografických systémů. Nakladatelství Československé Akademie Věd, Prague.

Kelly, M.A., Buoncristiani, J.-F., Schlüchter, C., 2004. A reconstruction of the last glacial maximum (LGM) ice-surface geometry in the western Swiss Alps and contiguous Alpine regions in Italy and France. Eclogae Geol. Helv. 97, 57–75. https://doi.org/10.1007/s00015-004-1109-6.

Krause, D., Margold, M., 2019. Glacial geomorphology of the Šumava / Bayerischer Wald mountains, Central Europe. J. Maps 15, 719–725. https://doi.org/10.1080/17445647.2019.1661881.

Křížek, M., Mida, P., 2013. The influence of aspect and altitude on the size, shape and spatial distribution of glacial cirques in the High Tatras (Slovakia, Poland). Geomorphology 198, 57–68. https://doi.org/10.1016/j.geomorph.2013.05.012.

Křížek, M., Vočadlová, K., Engel, Z., 2012. Cirque overdeepening and their relationship to morphometry. Geomorphology 139–140, 495–505. https://doi.org/10.1016/j.geomorph.2011.11.014.

MathWorks, 2019. MathWorks: MatLab documentation. https://www.mathworks.com/help/matlab/.

Mîndrescu, M., Evans, I.S., 2014. Cirque form and development in Romania: allometry and the buzzsaw hypothesis. Geomorphology 208, 117–136. https://doi.org/10.1016/j.geomorph.2013.11.019.

Mitchell, W.A., 1996. Significance of snowblow in the generation of Loch Lomond Stadial (Younger Dryas) glaciers in the western Pennines, northern England. J. Quat. Sci. 11, 233–248.

Mitchell, S.G., Humphries, E.E., 2015. Glacial cirques and the relationship between equilibrium line altitudes and mountain range height. Geology 43, 35–38. https://doi.org/10.1130/G36180.1.

Olyphant, G.A., 1977. Topoclimate and the depth of cirque erosion. Geogr. Ann. Ser. A 59, 209–213. https://doi.org/10.2307/520800.

Olyphant, G.A., 1981. Allometry and cirque evolution. Geol. Soc. Am. Bull. 92, 679–685. https://doi.org/10.1130/0016-7606(1981)92<679:AACE>2.0.CO;2.

Principato, S.M., Lee, J.F., 2014. GIS analysis of cirques on Vestfirðir, Northwest Iceland: implications for palaeoclimate: GIS analysis of cirques on Vestfirðir, NW Iceland. Boreas 43, 807–817. https://doi.org/10.1111/bor.12075.

Sanders, W.S., Cuffey, K.M., MacGregor, K.R., Collins, B.D., 2013. The sediment budget of an alpine cirque. Geol. Soc. Am. Bull. 125, 229–248. https://doi.org/10.1130/B30688.1.

Seguinot, J., Ivy-Ochs, S., Jouvet, G., Huss, M., Funk, M., Preusser, F., 2018. Modelling last glacial cycle ice dynamics in the Alps. Cryosphere 12, 3265–3285. https://doi.org/10.5194/tc-12-3265-2018.

Seif, A., Ebrahimi, B., 2014. Combined use of GIS and experimental functions for the morphometric study of glacial cirques, Zardkuh Mountain, Iran. Quat. Int. 353, 236–249. https://doi.org/10.1016/j.quaint.2014.07.005.

Sekyra, J, Sekyra, Z, 2002. Former existence of a plateau icefield in Bílá louka meadow, Eastern Giant Mountains: hypothesis and evidence/Předpoklady a důkazy existence náhorního (fjeldového) ledovce v oblasti Bílé louky (východní část Krkonoš). Opera Corcontica 39, 35–43.

Shala, S., Helmens, K.F., Luoto, T.P., Väliranta, M., Weckström, J., Salonen, J.S., Kuhry, P., 2014. Evaluating environmental drivers of Holocene changes in water chemistry and aquatic biota composition at Lake Loitsana, NE Finland. J. Paleolimnol. 52, 311–329. https://doi.org/10.1007/s10933-014-9820-4.

Smith, B., Varzi, A.C., 2000. Fiat and bona fide boundaries. Philos. Phenomenol. Res. 60 (2), 401–420. https://doi.org/10.2307/2653492.

Spagnolo, M., Pellitero, R., Barr, I.D., Ely, J.C., Pellicer, X.M., Rea, B.R., 2017. ACME, a GIS tool for automated cirque metric extraction. Geomorphology 278, 280–286. https://doi.org/10.1016/j.geomorph.2016.11.018.

Spagnolo, M., Rea, B.R., Barr, I., 2022. The (mis)conception of average Quaternary conditions. Quat. Res. 105, 235–240. https://doi.org/10.1017/qua.2021.48.

StatSoft, 2009. StatSoft: STATISTICA 9.0. https://www.statsoft.com.

Straumann, R.K., Purves, R.S., 2011. Computation and elicitation of valleyness. Spat. Cogn. Comput. 11, 178–204. https://doi.org/10.1080/13875868.2010.537797.

Tribe, A., 1991. Automated recognition of valley heads from digital elevation models. Earth Surf. Process. Landf. 16, 33–49. https://doi.org/10.1002/esp.3290160105.

Tribe, A., 1992. Problems in automated recognition of valley features from digital elevation models and a new method toward their resolution. Earth Surf. Process. Landf. 17, 437–454. https://doi.org/10.1002/esp.3290170504.

Turnbull, J.M., Davies, T.R.H., 2006. A mass movement origin for cirques. Earth Surf. Process. Landf. 31, 1129–1148. https://doi.org/10.1002/esp.1324.

Vilborg, L., 1984. The cirque forms of Central Sweden. Geogr. Ann. Ser. A 66, 41–77. https://doi.org/10.2307/520939.

Vočadlová, K., Petr, L., Žáčková, P., Křížek, M., Křížová, L., Hutchinson, S.M., Šobr, M., 2015. The Lateglacial and Holocene in Central Europe: a multi-proxy environmental record from the Bohemian Forest, Czech Republic. Boreas 44, 769–784. https://doi.org/10.1111/bor.12126.

Wick, L., 2000. Vegetational response to climatic changes recorded in swiss late Glacial lake sediments. Palaeogeogr. Palaeoclimatol. Palaeoecol. 159, 231–250. https://doi.org/10.1016/S0031-0182(00)00087-0.

Young, R., 2004. Amphitheatre. In: Goudie, A.S. (Ed.), Encyclopedia of Geomorphology. Routledge, London, p. 21.